

E9624
8-25-95

An Active Homopolar Magnetic Bearing With High Temperature Superconductor Coils and Ferromagnetic Cores

G.V. Brown, E. DiRusso and A.J. Provenza
Lewis Research Center
Cleveland, Ohio

Prepared for
MAG '95

cosponsored by the University of Virginia's Center for Magnetic Bearings and
Virginia's Center for Innovative Technology
Alexandria, Virginia, August 8-11, 1995



National Aeronautics and
Space Administration

AN ACTIVE HOMOPOLAR MAGNETIC BEARING WITH HIGH TEMPERATURE SUPERCONDUCTOR COILS AND FERROMAGNETIC CORES

G.V. Brown, E. Dirusso and A.J. Provenza
National Aeronautics and Space Administration
Lewis Research Center
Cleveland, Ohio 44135

ABSTRACT

A proof-of-feasibility demonstration showed that high temperature superconductor (HTS) coils can be used in a high-load, active magnetic bearing in liquid nitrogen. A homopolar radial bearing with commercially wound HTS (Bi 2223) bias and control coils produced over 200 lb (890 N) radial load capacity (measured nonrotating) and supported a shaft to 14000 rpm. The goal was to show that HTS coils can operate stably with ferromagnetic cores in a feedback controlled system at a current density similar to that in Cu in liquid nitrogen. Design compromises permitted use of circular coils with rectangular cross section. Conductor improvements will eventually permit coil shape optimization, higher current density and higher bearing load capacity.

The bias coil, wound with nontwisted, multifilament HTS conductor, required negligible power to carry its direct current. The control coils were wound with monofilament HTS sheathed in Ag. These dissipated negligible power for direct current (i.e., for steady radial load components). When an alternating current (AC) was added, the AC component dissipated power which increased rapidly with frequency and quadratically with AC amplitude. In fact at frequencies above about 2 Hz, the effective resistance of the control coil conductor actually exceeds that of the silver which is in electrical parallel with the oxide superconductor. This is at least qualitatively understandable in the context of a Bean-type model of flux and current penetration into a Type II superconductor. Fortunately the dynamic currents required for bearing stability are of small amplitude. These results show that while twisted multifilament conductor is not needed for stable levitation, twisted multifilaments will be required to reduce control power for sizable dynamic loads, such as those due to unbalance.

INTRODUCTION AND BACKGROUND

The state of the art of high temperature superconductors (HTS) has reached the point that one can purchase HTS coils that carry 1000 A turns in liquid nitrogen (LN₂), produce a few hundred gauss and are as small as copper coils operating in the same conditions. These are roughly the requirements for coils in active magnetic bearings. There are concerns about feasibility which center around the poor physical strength of the ceramic superconductors, their poor critical current density (J_c) at LN₂ temperature, the prospect of high dynamic losses in HTS control coils that must carry currents with frequency components of several hundred hertz and

the physical difficulties of handling the HTS conductors. These concerns have previously confined HTS magnetic bearing development to the passive variety.

There are two distinct motivations for using superconducting coils in magnetic bearings instead of normal coils. They are to save power and to reduce coil cross section because of higher allowable current density. At LN_2 temperature at this time only the Bi 2223 material can carry enough current in the self field of a small coil to compete with normal conductors. Further improvements are likely in HTS materials.

Under a NASA Lewis Research Center grant to the University of Wisconsin (Eyssa and Huang, 1990), a substantial increase of load capacity was predicted if HTS windings are used in magnetic bearings. Three approaches were studied analytically. In the first the usual ferromagnetic cores were retained, but higher current density than is possible with Cu was assumed, yielding higher load capacity by driving the cores into saturation. (Load capacity increases after core saturation because the field gradient at the rotor continues to grow, but at a slower rate since the stator core has already made its maximum contribution.) The second approach was to abandon the stator cores and use only stator coils. The third approach used HTS coils on both stator and rotor. The second and third approaches will lead to higher loads but will also require the conductors to tolerate higher stress. Furthermore at LN_2 temperature, the J_c of present conductors is severely reduced by the self field of a coil. Hence at present it is only feasible to use the first approach, which does not require high stress or high field strength in the coils.

PHYSICAL DESCRIPTION OF MAGNETIC BEARING

The homopolar radial bearing geometry with a separate bias coil was chosen. The chance for successful operation of the bias coil, which carries only direct current, was expected to be high. This would offer a saving of the majority of the power consumed in the bearing. Successful operation of the control coils, which must carry a combination of direct and alternating currents to produce steady and dynamic radial forces, was less assured. There was concern about the ability of the HTS composite to carry rapidly changing currents.

A drawing of the bearing is shown in Fig. 1. The overall bearing size is 18 cm o.d., 11.2 cm long with a 7.57 cm diameter journal. The bias coil encircles the ferromagnetic shaft. The flux passes through the shaft, through four air gaps to the poles of one stator, to the exterior flux tube to the other stator and through that stator's air gaps to the rotor. We used only four control coils to reduce expense, installing them on one stator and leaving the other stator poles empty. The bias field at the empty poles contributes a negative stiffness. For flexible shaft modes this force may not be counteracted by the control forces at the other stator. It appeared prudent to use only circular coils at this stage of HTS conductor development. We therefore compromised the design of the other bearing parts to accommodate externally-wound, commercially-purchased, circular coils.

This bearing could also be operated as a four-pole heteropolar radial bearing if four power amplifiers were used and the bias current were carried in the "control" coils in addition to the control currents. (This might reduce unwanted magnetization currents in the superconductor due to a reduced margin between the steady current and the critical current.) Since we have no control coils at one end of the bearing, the negative stiffness due to those poles would be removed. This "advantage" is peculiar only to this particular geometry.

This bearing can be operated at room temperature because of the silver matrix in the coils. Several bearing performance measurements were made at room temperature before using LN_2 .

However, the allowable steady current in the coils at room temperature is limited by heating to about half of what is possible when the coils are superconducting. All data presented in this report was taken at LN₂ temperature.

THE HIGH TEMPERATURE SUPERCONDUCTING COILS

BIAS COIL

The bias coil in a homopolar radial magnetic bearing produces a steady magnetic field in the air gaps. The gap between the journal and stator is 0.5 mm. Since there are two gaps in series in the magnetic circuit, about 1000 A-turns are required to produce 1 T in the gaps, when allowing for leakage and fringing.

The commercially-produced circular bias coil (electrical size: 8.3 cm i.d., 11.8 cm o.d. and 1.36 cm long) was layer-wound on an aluminum coil form. A single length of multifilament conductor (19 filaments in a 0.2 by 2.5 mm Ag tape) was reacted before winding on the coil form. The silver-to-superconductor ratio is about 3. The 244 turn coil has a critical current, determined by the 1 μ V/cm criterion, of 3.9 A. The coil could be operated at 4.7 A with less than 20 mV potential drop. The coil without a ferromagnetic core produces a calculated maximum axial magnetic induction of ~400 G at its inner bore. The voltage across the coil versus steady current through the coil is shown in Fig. 2. The voltage was measured with voltage taps attached to the superconducting composite tape inside the current leads. The measured steady power dissipated in the coil versus current is shown in Fig. 3. This measurement was made in the rig (with ferromagnetic cores). Also shown is the power that would be required if only the Ag matrix were present. This gives a rough estimate of the power saved by using the HTS composite. However, the packing fraction (~52 percent) of the HTS tape in this rather short, layer-wound coil is lower than that possible with Cu or Ag wire.

CONTROL COILS

The control coils in a homopolar magnetic bearing with a separate bias coil must each provide about half the number of ampere-turns (500 A-t) as the bias coil (1000 A-t). This allows the two control coils on an axis to double the strength of one pole (in the absence of core saturation) and to reduce the strength of the opposite pole to zero. This gives the maximum net radial force toward the double-strength pole. The control coil must carry a combination of DC and AC currents to support steady loads (such as shaft weight) and dynamic loads (such as those due to shaft unbalance). We designed the control coils with 1000 A-t to allow heteropolar operation, if desired.

The four commercially-produced circular control coils were 3.6 cm i.d., 6.2 cm o.d. and 2.0 cm long. They were layer-wound from a single length of Ag tape (tape cross section 0.11 by 4.7 mm) with a monofilament HTS core and reacted after winding. The epoxy-impregnated coils fit over the laminated stator poles without any coil form to conserve space and to avoid eddy currents. Each coil has between 230 and 232 turns, and the critical currents (1 μ V/cm criterion) varied from 4.5 A to 5.6 A.

The voltage across one control coil as a function of steady current is shown in Fig. 4. The voltage was measured with taps on the Ag tape leads. The voltage increase at low currents comes partly from those leads, but it increases faster than linearly. The nonlinear part may be

due to segments of superconductor with reduced critical currents, which force current into the Ag. (The small jog in the curve near 5 A was caused by an instrumentation change.) The coil reached 5.8 A with under 8 mV potential drop.

The measured power dissipated at LN₂ temperature in two of the control coils is shown in Fig. 3, as well as the power calculated for a pair of coils if only the Ag were present. Note the ordinate log scale. The HTS power is seen to be two to three orders of magnitude lower for steady current, which would be required in control coils to support steady loads such as the weight of a horizontal shaft.

ALTERNATING CURRENT LOSS MEASUREMENTS ON CONTROL COILS

Control coil power dissipation was measured for single frequencies, with and without superimposed direct current, and with and without ferromagnetic cores. The average power P_{av} was obtained from the product of the coil current I and the coil voltage V , sampled at 12.8 kHz and averaged over a time T much larger than the period of the alternating current (AC) frequency f

$$P_{av} = (1/T) \int_0^T V(t) I(t) dt \quad (1)$$

where $T \gg 1/f$ and $I = I_0 \sin(2\pi ft)$. For any single frequency an effective resistance R_{eff} can be calculated by

$$R_{eff} = 2P_{av} / I_0^2. \quad (2)$$

We compare this effective resistance below to the calculated resistance of the Ag matrix at LN₂ temperature. That resistance is based on the measured room temperature resistance divided by 5.97 (the room temperature resistivity of Ag divided by its LN₂ temperature resistivity).

AIR CORE LOSSES

The average power dissipated in one of the control coils as a function of frequency with no DC offset current for several current amplitudes I_0 was measured. The effective resistance, calculated from the results by using Eqs. (1) and (2), is shown in Fig. 5. One can see from this figure, which shows the Ag matrix resistance for comparison, that the resistance of the HTS composite surpasses the Ag resistance above about 100 Hz. The coils would have less resistance above that frequency if the oxide were not present! This result is not so surprising if one thinks of flux penetration into the superconductor on a Bean-type model (Bean, 1964). The currents and fields cannot freely penetrate the entire cross section of the composite tape, but must enter from surfaces as the current and field increase, rather like (but not the same as) a skin depth effect. Hence at high enough frequency, induced supercurrents prevent parts of the Ag from carrying transport current, increasing the apparent resistance. This problem will be reduced by twisted multifilamentary conductor, which is well developed for low temperature superconductors but is beyond the present HTS art.

The effect of DC offset current added to AC is shown in Fig. 6. There the frequency is fixed at 25 Hz and data for AC amplitude values of 0.5, 1 and 2 A are shown. At this frequency the effect of DC offset is relatively minor and appears to be mainly due to the increase in resistance

seen without any superimposed AC component. The measured power actually decreased with DC offset for an AC amplitude of 2 A. One possible explanation is that the DC offset may reduce the ability of the composite conductor to support shielding currents, allowing a greater portion of the Ag to carry transport current.

AC losses in the absence of DC offset current, measured for all the control coils outside of the bearing without ferromagnetic cores, are shown in Fig. 7. Throughout the rest of the AC results, the symbols are consistent from graph to graph. The circles are for the coil used on the -X pole, diamonds for +X, triangles for -Y and squares for +Y. There are substantial differences between coils, which is not surprising at this stage of HTS conductor and coil technology. All AC results before Fig. 7 were for the -X coil, one of the lowest loss coils. The +X coil stands out as significantly worse than the others at high frequencies.

AC LOSSES WITH FERROMAGNETIC CORE

The effective resistance of all of the control coils was then measured in the magnetic bearing for pure frequencies. The results are shown in Fig. 8. The increase in resistance occurs at much lower frequencies than it did without ferromagnetic cores. The +X coil is again much worse than the others.

With cores the resistance surpasses the Ag resistance at about 2 Hz rather than 60 to 100 Hz. This is not surprising because the flux change through the coils is much greater. The behavior of the resistance in the two cases with respect to frequency is remarkably similar with a simple change of frequency scale. Figure 9 shows the two sets of data plotted together but with the frequencies of the air-core results divided arbitrarily by 50 (a number selected to best superimpose the two sets of data). There is considerable correspondence between the results for the same coil, with and without cores. Inductance measurements were made on the coils between 1 and 10 Hz in the superconducting state with and without the ferromagnetic cores. Those measurements yielded 75 and 2.2 mH, respectively. The ratio of these values is 34, a number of the same order of magnitude as the value of 50 used above to rescale the air-core frequency data. These results suggest that the losses can be largely linked to the rate of flux change through the coils. It is therefore hoped that twisted, multifilamentary conductor will substantially reduce the losses, making their onset occur at higher frequency and limiting their maximum values to approximately what would occur in the Ag.

CONTROL COIL POWER DISSIPATION WITH ROTATING SHAFT

The power dissipated in the control coils was measured at various constant speeds of the rotor, with the rotor in its best balance condition and with 0.095 oz-in. of unbalance. The spectral content of the control current with the rotor spinning is much more complex than in the single-frequency tests of the previous sections. The shaft rotating frequency ranged from 0 to 160 Hz during loss measurements. Imperfections in the sensing surface for the position probes introduce multiples of the rotating frequency. Furthermore the derivative gain in the PID controller amplifies noise in proportion to its frequency. The rotating results are shown in Fig. 10. The +X coil is again generally the worst. The -Y coil, as previously, is next worst. The Y axis generally had less stability margin than the X.

We may hope that the losses measured for the better coils represent upper bounds for what will be possible for monofilament conductor as its technology improves. Twisted multifilamentary conductor should provide substantial reduction from that level.

MAGNETIC BEARING OPERATING RESULTS

The LN₂ test rig has been described previously (DiRusso and Brown, 1992; DiRusso, Brown and Provenza, 1994). The shaft is vertical, supported near the top by a conventional ball bearing pair operating at room temperature. The magnetic bearing near the lower end of the shaft can be submerged in LN₂.

The bearing was operated to the maximum speed of the rig, 14,000 rpm, both at room temperature at 2 A bias and at LN₂ temperature at various bias currents up to 4 A. For stable operation it was necessary to use values of damping several times as high as required for other bearings we have run of similar size. At this time we do not know if this is caused by the superconducting coils, the uncontrolled stator poles, or another cause.

A maximum load capacity of 200 lb (890 N) was produced by the bearing, as shown in Fig. 11, and the linear load range (during load increase) is about 125 to 150 lb (556 to 668 N). The figure shows complete force hysteresis loops (each taken over a 5 sec period) for maximum control currents of ± 4 and ± 2 A. The higher current carries the force to a saturation level. The hysteresis is probably due to the Co-Fe core material rather than to superconducting effects. Closed magnetization currents in the coils do not encircle the ferromagnetic core and hence cannot affect the magnetomotive force in the magnetic circuit. Loads were measured with the shaft nonrotating with a load fixture with small load cells.

With approximately 3 cm increase in bearing length, control coils could be added to the empty stator, increasing the maximum load capacity to 400 lb (1780 N).

BASIC MAGNETIC BEARING OPERATING PARAMETERS

The dependence of bias force on shaft displacement for various bias coil current levels (no control coil current) is shown in Fig. 12. The slopes of these curves give the negative stiffness of the bearing. The values near zero displacement are 3.8, 5.2 and 6.5 lb/mil (666, 911 and 1140 N/mm) for 2, 3 and 4 A bias current, respectively. The actuator gain, the slope of the force versus control current curves shown in Fig. 11, is about 77 lb/A (343 N/A) near zero current.

At LN₂ temperature we measured a bearing force as a function of shaft displacement in closed loop operation. The highest stiffness that we measured was 17.5 lb/mil (3070 N/mm) (see $k = 10$, $c = 5$ curves of Fig. 13). The stiffness during our rotating loss measurements was only 5.8 lb/mil (1020 N/mm) ($k = 5$, $c = 5$ curves of Fig. 13).

CONTROLLER

The bearing was controlled during high speed runs by a digital controller, written in Turbo Pascal and run in the CPU of a 66 Mhz 486 PC, with a loop time of about 50 μ -sec. Four position probe inputs and a 1-per-rev pulse are sampled in each loop by a plug-in A/D card, the two control outputs are calculated and the results are sent to a D/A plug-in card. The controller is a PD controller with an adjustable bandwidth limit.

For the rotating AC loss measurements an analog controller was used, which for the same low-frequency stiffness and damping, had lower high frequency noise than the digital controller. (This is not to be taken as a problem with digital controls in general, only our particular implementation.)

CONCLUSIONS AND FUTURE NEEDS

We have shown that an active high-load HTS magnetic bearing can be operated at LN_2 temperature with several performance measures approaching those possible with conventional windings. Comparable current density and hence coil size were obtained. At lower temperature (e.g., liquid hydrogen temperature) the coils could be substantially smaller, subject to stress limitations, of course. Power to supply the bias field was reduced essentially to zero, the same advantage provided by permanent magnet biasing. Power dissipated in the control coils to support steady loads was reduced essentially to zero. The control coils support dynamic currents sufficiently well to permit stable levitation up to the top speed (14,000 rpm) of our rig. A.C. losses appear to be related to coil inductance, suggesting that a twisted multifilamentary conductor could reduce the losses substantially.

We found that the power dissipated in the control coils above about 2 Hz exceeded that which would be dissipated in normal coils (by several times in the best coils and by over an order of magnitude in the worst).

Critical currents of the HTS conductors are improving and smaller coils are already possible. The primary technical improvements needed for active bearings that retain ferromagnetic cores are the ability to wind noncircular coils and, most importantly, the development of a twisted, multifilamentary conductor.

REFERENCES

Eyssa, Y.M. and X. Huang, "High Pressure Superconducting Radial Magnetic Bearing," IECEC-90, Proceedings of the 25th Intersociety Energy Conversion Engineering Conference, Reno, Nev., Aug. 12-17, 1990. Vol. 3. New York, American Inst. of Chem. Engin., 1990. Work performed under NASA grant NAG3-1041.

Bean, C.P., Rev. Mod. Phys., 36, 31 (1964).

DiRusso, E. and G. V. Brown, "Performance Tests of a Cryogenic Hybrid Magnetic Bearing for Turbopumps," Proceedings of the Third International Symposium on Magnetic Bearings, Paul Allaire, editor, p. 386, Technomic Publishing Company, Inc., Lancaster, PA, 1992.

DiRusso, E., G. V. Brown, and A. J. Provenza, "Tests of a Cryogenic Electromagnet Biased Homopolar Magnetic Bearing," Advanced Earth-to-Orbit Propulsion Technology - 1994, NASA Conference Publication 3282, Vol. II, p. 385, 1994.

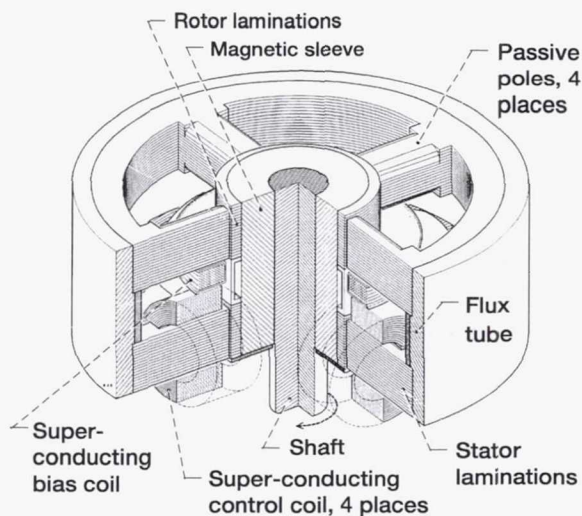


Figure 1.—Drawing of active HTS magnetic bearing.

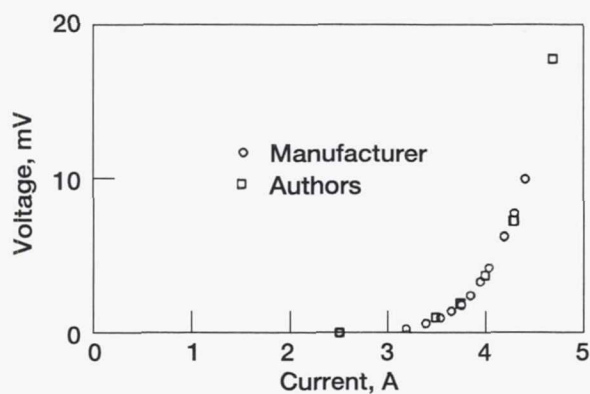


Figure 2.—Voltage across bias coil as a function of steady current at LN₂ temperature.

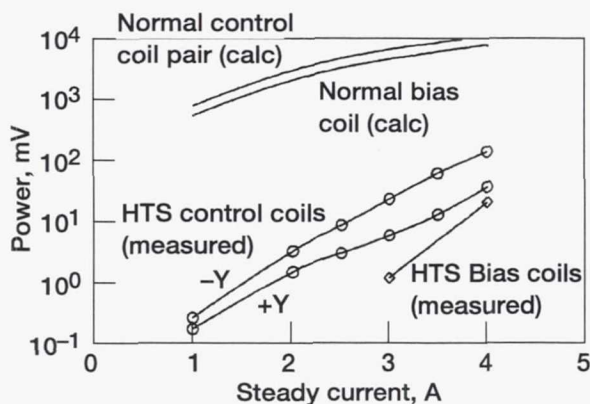


Figure 3.—Comparison of power consumption of HTS coils with normal coils (based on Ag cross sections in coils).

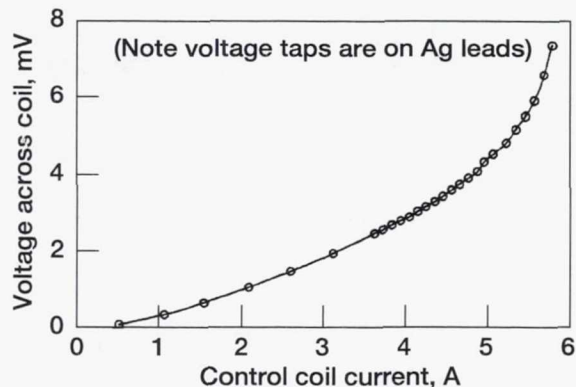


Figure 4.—Onset of voltage in control coil for steady current.

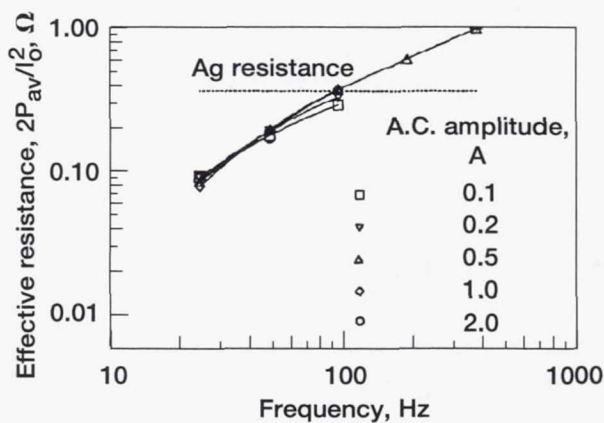


Figure 5.—Effective resistance of control coil as a function of frequency for several values of AC amplitude with no DC offset.

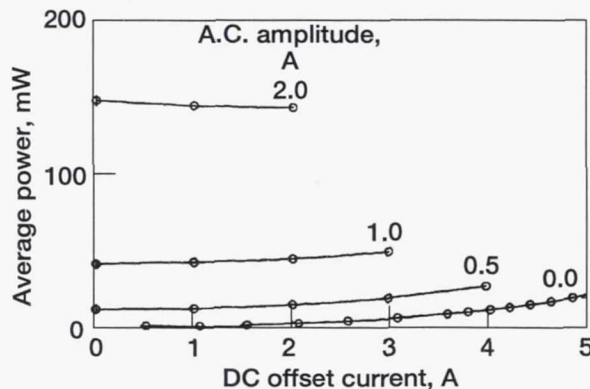


Figure 6.—Average control coil power as a function of DC offset at 25 Hz for four values of AC amplitude.

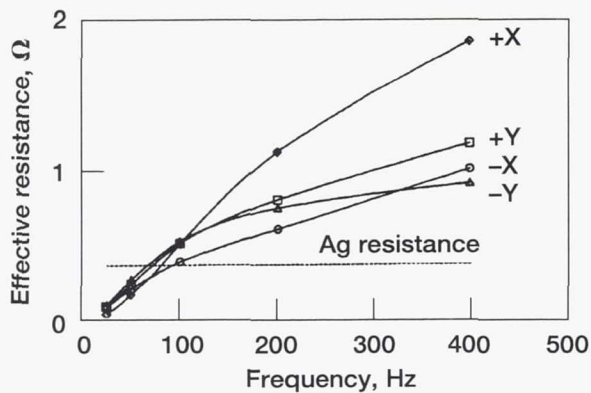


Figure 7.—Effective resistance of control coils as a function of frequency at 0.5 A amplitude with no DC offset without ferromagnetic core.

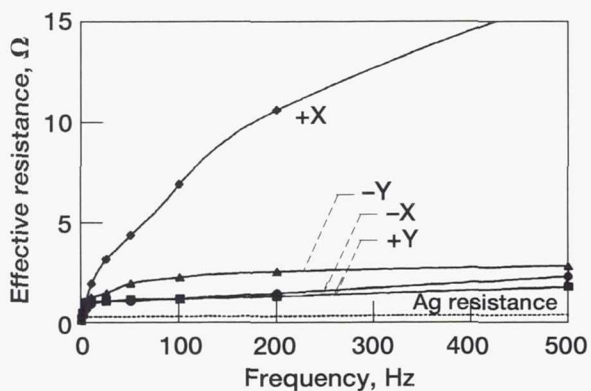


Figure 8.—Effective resistance of control coils as a function of frequency with ferromagnetic cores (in rig) for 0.5 A AC amplitude and no DC offset.

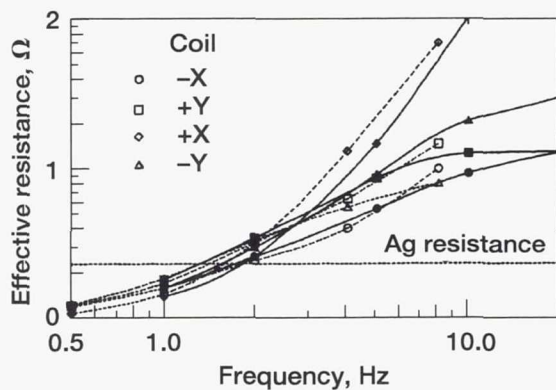


Figure 9.—Effective resistance vs frequency for control coils with cores (filled symbols) and vs frequency divided by 50 for coils without cores (open symbols). AC amplitude is 0.5 A.

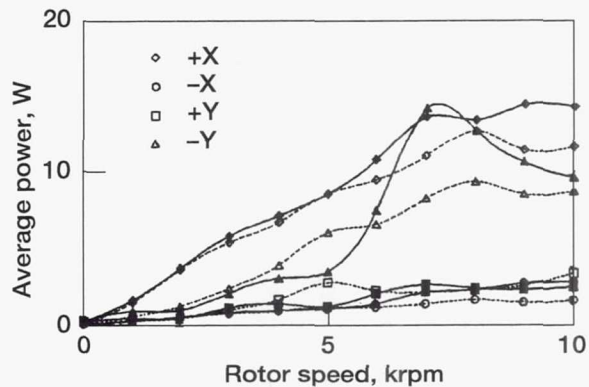


Figure 10.—Control coil power dissipation vs rotor speed, balanced (open symbols) and with 0.095 oz-in unbalance (filled symbols). Bias = 4 A, $k = 5$, $c = 5$.

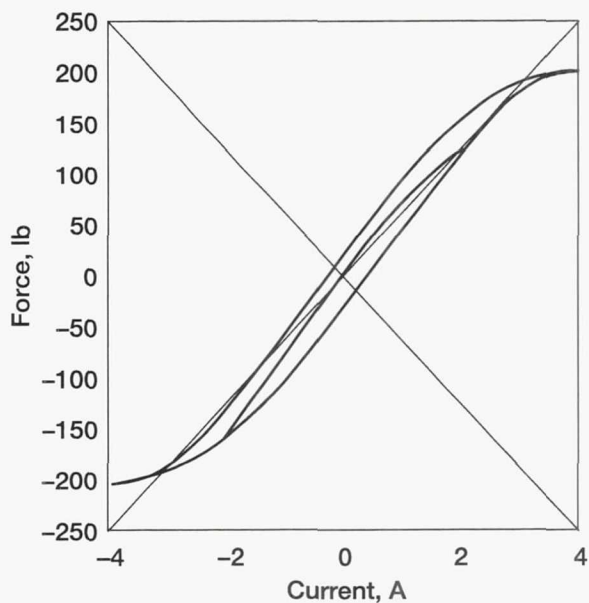


Figure 11.—Bearing force as a function of control current at 4 A bias current. X axis, liquid nitrogen temperature.

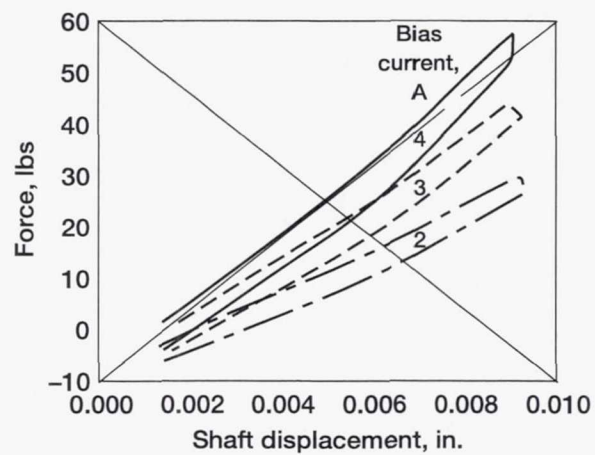


Figure 12.—Bias force as a function of shaft displacement. X axis, liquid nitrogen temperature.

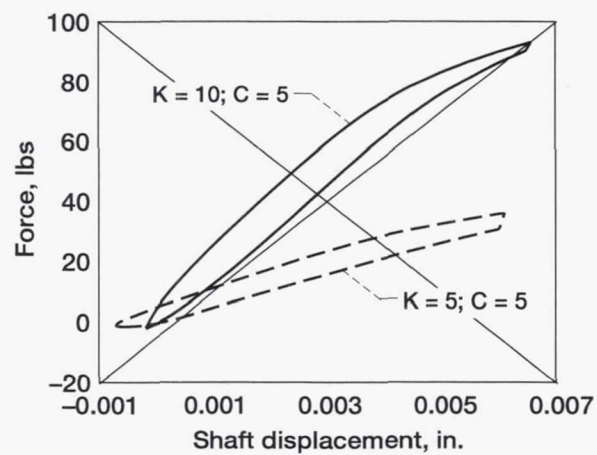


Figure 13.—Bearing force vs. shaft displacement for two values of proportional gain. Bias current is 4 A. X axis, liquid nitrogen temperature.

REPORT DOCUMENTATION PAGE

OMB No. 0704-0188

Public reporting burden for this collection of information is estimated to average 1 hour per response, including the time for reviewing instructions, searching existing data sources, gathering and maintaining the data needed, and completing and reviewing the collection of information. Send comments regarding this burden estimate or any other aspect of this collection of information, including suggestions for reducing this burden, to Washington Headquarters Services, Directorate for Information Operations and Reports, 1215 Jefferson Davis Highway, Suite 1204, Arlington, VA 22202-4302, and to the Office of Management and Budget, Paperwork Reduction Project (0704-0188), Washington, DC 20503.

1. AGENCY USE ONLY (Leave blank)		2. REPORT DATE August 1995		3. REPORT TYPE AND DATES COVERED Technical Memorandum	
4. TITLE AND SUBTITLE An Active Homopolar Magnetic Bearing With High Temperature Superconductor Coils and Ferromagnetic Cores				5. FUNDING NUMBERS WU-505-63-5B	
6. AUTHOR(S) G.V. Brown, E. DiRusso, and A.J. Provenza					
7. PERFORMING ORGANIZATION NAME(S) AND ADDRESS(ES) National Aeronautics and Space Administration Lewis Research Center Cleveland, Ohio 44135-3191				8. PERFORMING ORGANIZATION REPORT NUMBER E-9624	
9. SPONSORING/MONITORING AGENCY NAME(S) AND ADDRESS(ES) National Aeronautics and Space Administration Washington, D.C. 20546-0001				10. SPONSORING/MONITORING AGENCY REPORT NUMBER NASA TM-106916	
11. SUPPLEMENTARY NOTES Prepared for MAG'95 cosponsored by the University of Virginia's Center for Magnetic Bearings and Virginia's Center for Innovative Technology, Alexandria, Virginia, August 8-11, 1995. Responsible person, G.V. Brown, organization code 5230, (216) 433-6047.					
12a. DISTRIBUTION/AVAILABILITY STATEMENT Unclassified - Unlimited Subject Categories 31 and 37 This publication is available from the NASA Center for Aerospace Information, (301) 621-0390.				12b. DISTRIBUTION CODE	
13. ABSTRACT (Maximum 200 words) A proof-of-feasibility demonstration showed that high temperature superconductor (HTS) coils can be used in a high-load, active magnetic bearing in liquid nitrogen. A homopolar radial bearing with commercially wound HTS (Bi 2223) bias and control coils produced over 200 lb (890 N) radial load capacity (measured non-rotating) and supported a shaft to 14000 rpm. The goal was to show that HTS coils can operate stably with ferromagnetic cores in a feedback controlled system at a current density similar to that in Cu in liquid nitrogen. Design compromises permitted use of circular coils with rectangular cross section. Conductor improvements will eventually permit coil shape optimization, higher current density and higher bearing load capacity. The bias coil, wound with non-twisted, multifilament HTS conductor, required negligible power to carry its direct current. The control coils were wound with monofilament HTS sheathed in Ag. These dissipated negligible power for direct current (i.e. for steady radial load components). When an alternating current (AC) was added, the AC component dissipated power which increased rapidly with frequency and quadratically with AC amplitude. In fact at frequencies above about 2 hz, the effective resistance of the control coil conductor actually exceeds that of the silver which is in electrical parallel with the oxide superconductor. This is at least qualitatively understandable in the context of a Bean-type model of flux and current penetration into a Type II superconductor. Fortunately the dynamic currents required for bearing stability are of small amplitude. These results show that while twisted multifilament conductor is not needed for stable levitation, twisted multifilaments will be required to reduce control power for sizable dynamic loads, such as those due to unbalance.					
14. SUBJECT TERMS Magnetic bearings; High temperature superconductors; Active magnetic bearings; Superconducting magnetic bearings				15. NUMBER OF PAGES 12	
				16. PRICE CODE A03	
17. SECURITY CLASSIFICATION OF REPORT Unclassified	18. SECURITY CLASSIFICATION OF THIS PAGE Unclassified	19. SECURITY CLASSIFICATION OF ABSTRACT Unclassified	20. LIMITATION OF ABSTRACT		